2006

Trans-10, cis-12 conjugated linoleic acid causes inflammation and delipidation of white adipose tissue in mice: a microarray and histological analysis

P. Christopher LaRosa
University of Nebraska - Lincoln, plarosa1@unl.edu

Jess L. Miner
University of Nebraska - Lincoln, jminer1@unl.edu

Yuannan Xia
University of Nebraska - Lincoln

You Zhou
University of Nebraska-Lincoln, yzhou2@unl.edu

Stephen D. Kachman
University of Nebraska-Lincoln, steve.kachman@unl.edu

See next page for additional authors

Physiol Genomics 27: 282–294, 2006.
First published July 25, 2006; doi:10.1152/physiolgenomics.00076.2006.

Trans-10, cis-12 conjugated linoleic acid causes inflammation and delipidation of white adipose tissue in mice: a microarray and histological analysis

P. Christopher LaRosa,[1] Jess Miner,[2] Yuannan Xia,[1] You Zhou,[1] Steve Kachman,[3] and Michael E. Fromm[1]

[1]*Center for Biotechnology,* [2]*Department of Animal Science, and* [3]*Department of Statistics, University of Nebraska, Lincoln, Nebraska*

Submitted 1 May 2006; accepted in final form 21 July 2006

LaRosa, P. Christopher, Jess Miner, Yuannan Xia, You Zhou, Steve Kachman, and Michael E. Fromm. Trans-10, cis-12 conjugated linoleic acid causes inflammation and delipidation of white adipose tissue in mice: a microarray and histological analysis. *Physiol Genomics* 27: 282–294, 2006. First published July 25, 2006; doi:10.1152/physiolgenomics.00076.2006.—A combined histological and microarray analysis of the white adipose tissue (WAT) of mice fed *trans*-10, *cis*-12 conjugated linoleic acid (t10c12 CLA) was performed to better define functional responses. Mice fed t10c12 CLA for 14 days lost 85% of WAT mass, 95% of adipocyte lipid droplet volume, and 15 or 47% of the number of adipocytes and total cells, respectively. Microarray profiling of replicated pools ($n = 2$ per day × diet) of control and treated mice ($n = 140$) at seven time points after 1–17 days of t10c12 CLA feeding found between 2,682 and 4,216 transcript levels changed by twofold or more. Transcript levels for genes involved in glucose and fatty acid import or biosynthesis were significantly reduced. Highly expressed transcripts for lipases were significantly reduced but still abundant. Increased levels of mRNAs for two key thermogenesis proteins, uncoupling protein 1 and carnitine palmitoyltransferase 1, may have increased energy expenditures. Significant reductions of mRNAs for major adipocyte regulatory factors, including peroxisome proliferator activated receptor-γ, sterol regulatory binding protein 1, CAAT/enhancer binding protein-α, and lipin 1 were correlated with the reduced transcript levels for key metabolic pathways in the WAT. A prolific inflammation response was indicated by the 2- to 100-fold induction of many cytokine transcripts, including those for IL-6, IL-1β, TNF ligands, and CXC family members, and an increased density of macrophages. The mRNA changes suggest that a combination of cell loss, increased energy expenditure, and residual transport of lipids out of the adipocytes may account for the cumulative mass loss observed.

lipid metabolism; gene expression; cell biology

DIETARY CONJUGATED LINOLEIC ACID (CLA), either as mixed isomers or the specific trans-10, cis-12 isomer (t10c12 CLA), dramatically reduces fat content in white adipose tissues (WAT) in mice (10, 36) although results in humans have been inconsistent (51, 52). Weight losses in WAT of up to 70% have been reported in mice on diets containing 0.5–1% CLA (10, 50). In mice this reduction is due to altered energy metabolism or transport and is not generally due to reduced feed intake (10, 17, 49, 51, 53, 54). CLA increases energy expenditure in whole mice and is correlated with increases in the mRNAs for mitochondrial uncoupling protein 1 and 2 (UCP1, UCP2) in some studies (21, 47, 50) but not others (53). Proinflammatory cytokines levels, including those of tumor necrosis factor (TNF-α) and interleukins 6 and 8 (IL-6 and IL-8) are increased in response to CLA (4, 50).

At the cellular level, evidence supports either apoptotic loss of cells (11, 18, 34, 50) or reduced triglyceride (TG) content in surviving adipocytes (11, 50). Cumulative cellular TG levels respond to changes in the balance of the cellular energy import, export, or expenditure. Transcripts of genes involved in glucose import and fatty acid biosynthesis are reduced in CLA-treated cells (47, 50). Key metabolic genes that are downregulated by CLA include glucose transporter 4 (Glut4), acetyl-CoA carboxylase, and fatty acid synthase, whereas key regulatory genes that are downregulated include sterol regulatory binding protein 1 (SREBP1), peroxisome proliferator activated receptor (PPAR)-γ, and CCAAT/enhancer binding protein (C/EBP)-α (see Ref. 22 for a recent review). Microarray analyses of the genomic response of polygenic obese and control mice generally confirmed the above observations at the level of gene expression 5 and 14 days after CLA treatment in adipose tissues (21). Despite the considerable progress at describing the molecular responses to CLA its primary site of action is still unknown.

In the present studies, we analyzed the retroperitoneal (RP) WAT of C57BL/6J mice fed t10c12 CLA for times ranging from 1 to 17 days. Cellular and gene expression changes were determined using histological examination and microarrays capable of detecting ~34,000 transcripts. Delipidation and cell loss both occurred, and up to 4,216 transcript levels changed by twofold or more ($P < 0.01$). These genes were grouped into biochemical and signaling pathways to explain the cellular changes observed in the WAT.

MATERIALS AND METHODS

Animals

All animal experiment protocols (#03-06-021) were reviewed and approved by the Institutional Animal Care and Use Committee of University of Nebraska-Lincoln and followed National Institutes of Health guidelines for the Care and Use of Laboratory Animals (Publications No. 80-23; revised in 1996). We housed 152 9-wk-old male C57BL/6J mice (Charles River Laboratories) individually and fed them pellets of modified AIN-93G (soy protein replaces casein, Dyets) diet for 11 days before treatment initiation. Treatments were either control diet AIN-93G or t10c12 CLA diet consisting of control diet with 0.5% of the soy oil substituted with 0.5% t10c12 CLA (Nu-Chek Prep, Elysian, MN). Mice were allowed to feed ad libitum until death by CO_2 asphyxiation. We killed 20 mice on each of *days 1, 2, 3, 4, 7, 10,* and *17*. Both epididymal (EP) and RP fat pads were excised, weighed, and then frozen in liquid nitrogen for subsequent mRNA analyses. Twelve mice were killed on *day 14* to obtain tissue for histological analyses as described later. The weight and feed data

Article published online before print. See web site for date of publication (http://physiolgenomics.physiology.org).

Address for reprint requests and other correspondence: M. E. Fromm, Ctr. for Biotechnology, 1901 Vine St, Lincoln, NE 68588-0665 (e-mail: mfromm@unlnotes.unl.edu).

were analyzed with the PROC MIXED procedure of SAS (SAS Inst., 2003) as a 7 × 2 factorial with heterogeneous variances across days. The model included main effects for days and treatment along with the day by treatment interaction. Contrasts were used to compare control and t10c12 CLA-fed mice within day.

Histological and Immunofluorescence Microscopy and Quantitative Image Analysis

Each pair of the RP tissues from mice fed either control or t10c12 CLA diets for 14 days (six mice for each control and treatment group) was isolated, weighed, and immediately fixed for quantitative image and immunochemical analyses. One of the two RP tissues from each of the mice was fixed in 3.7% formaldehyde in PBS and processed for paraffin embedding, sectioning, and standard hematoxylin and eosin (H&E) staining. These H&E-stained sections were used for quantitative measurement of the mean diameters of adipocytes. The number of adipocytes, defined as the cells containing empty areas from which the fat contents were removed during the dehydration process, in a fixed area was counted, and the cell diameter was determined from sections of each individual RP section for a total of 63 images each for control and treated samples, using a SoftImaging image analysis program (Olympus).

The other RP fat pad from each mouse was fixed in 2.5% glutaraldehyde in PBS, washed, and stained with 1% Sudan black dye (for visualizing the fat content) in PBS containing 0.5% Triton X-100 at room temperature for 3 h. This set of RP tissues was washed in PBS and stained with 2 μM Sytox green (for visualizing the DNA in the nucleus) in PBS containing 0.5% Triton X-100 overnight at 4°C. The stained sections were then used for quantitative comparison of numbers of cells, as determined by the density of the stained nuclei in a given volume, in each of the RP tissues.

To determine the cell density of the RP tissues a series of 512 × 512 frames from confocal optical images was collected with a ×10 lens using a *Z*-step of ~5 μm for ~40–50 μm in depth using an Olympus FV confocal laser scanning system on an IX80 inverted microscope. Dual laser lines were used to collect two color images simultaneously: a 405-nm line was used for fluorescence of fat content stained with Sudan black dye and a 488-nm line for Sytox green-stained nuclei. Final extended focusing images (four from the larger control tissues and three from the smaller treatment tissues for each mouse RP tissue) covering 1,200 μm × 400 μm × 40 μm regions of the RP tissues were used for quantitative image analysis with a SoftImaging image analysis program (Olympus). The numbers of nuclei within the areas of fluorescence were determined from each image, and an average cell density was obtained from 24 control images and 18 treated images.

For immunofluorescence labeling of macrophages, paraffin sections from the same adipose tissues used for morphological analysis were processed for conventional immunofluorescence labeling using rat antibodies to mouse CD68 (1:50 dilution; Serotec, Raleigh, NC), a known marker for monocytes and macrophages. Cy5-conjugated goat anti-mouse IgG secondary antibodies (Jackson ImmunoResearch, West Grove, PA) were used for fluorescence detection of the CD68, and a DNA-staining fluorescent dye Sytox green (Molecular Probes) was used for nuclear counterstain. We collected 50 images from each group (control and t10c12 CLA-treated), and CD68-labeled cells were counted and averaged.

RNA Isolation and Labeling

RNA for each time point was isolated from two control and two treatment samples for analysis on four microarrays. The two control and two treatment samples consisted of RP tissues from five pooled mice for each sample, requiring a total of 20 mice for the four samples taken at each time point. Total RNA was extracted from the frozen RP tissues of each sample using TRIzol (Invitrogen) reagent. We used 15 μg of total RNA to produce labeled cRNA for hybridization to Affymetrix GeneChip Mouse Genome 420 2.0 arrays with the manufacturer's protocols (Affymetrix).

Microarray Data Analysis

Affymetrix GeneChip Operating Software generated the image and probe set signal values as cel files, and the cel files were processed with the *affy* package (13) using the robust multiarray analysis (RMA, Ref. 24) to generate normalized signal values. The RMA signal values were log2 transformed. The arrays were screened for outlying arrays by plotting the $M = (X - Y)$ and $A = (X + Y)/2$ values for pairs of arrays where X and Y are the transformed RMA expression values. One of the *day 2* control arrays was inconsistent with the other arrays on *day 2* and that array was removed from further analysis. To detect differentially expressed genes the transformed RMA expression values were analyzed with an empirical Bayes linear model (45, 46). The linear model included fixed effects for days and treatment nested within days. A gene was viewed as differentially expressed on a given day either if it had a large effect on that day or if it had a consistent effect with an adjacent day. A single day effect was quantified by the moderated *t*-statistic for the treatment effect on that day. A consistent effect with 2 days was quantified as the minimum moderated *t*-statistic for the 2 days. A consistent effect between adjacent days was then defined to be the maximum of the effects for a day before and the day after. A *P* value for a gene being differentially expressed on a day was then calculated as the probability of obtaining a value smaller than the observed minimum of the single day *P* value and the consistent effect *P* value if the gene was not differentially expressed. A gene was considered differentially expressed if the false discovery rate-adjusted *P* value was <5%. The series record of the data submitted to the National Center for Biotechnology Information Gene Expression Omnibus is GSE4671.

Pathway analysis. The sorted lists of up- and downmodulated genes containing the Affymetrix probe set identifiers and their averaged signal log ratios (log2) were entered into the Ingenuity Pathway Analysis software (Ingenuity Systems, www.ingenuity.com) to help organize them into known biological pathways. When probe sets redundantly represented a single gene, the probe set with the maximum signal log ratio was used in the analysis. Probability scores for each network or functional grouping are calculated as to the chances of the mRNA abundance changes predicting these interactions and networks. A full discussion of the statistical methodologies employed can be found in the supplemental files of Calvano et al. (6).

Quantitative RT-PCR. First-strand cDNA synthesis used Moloney murine leukemia virus reverse transcriptase and 0.5 μg of total RNA primed with oligo $(dT)_{17}$ (Invitrogen). The single-strand cDNA pool was diluted 10- to 100-fold and used as template for quantitative real-time PCR. Relative levels of the target mRNAs were determined using a Bio-Rad iCycler iQ and the iQ SYBR Green Supermix reagent. The target mRNA was normalized relative to the levels of the housekeeping gene β2-microglobulin.

RESULTS

T10c12 CLA Causes Significant Loss of Adipose Tissue Without Body Weight Loss or Reduced Feed Intake

Neither body weight nor feed intake was influenced by t10c12 CLA (Fig. 1*A* and Supplemental Fig. 1; the online version of this paper contains supplemental data). Conversely, weights of the RP and EP fat pads from t10c12 CLA-fed mice were <25% of the control (Fig. 1*B*).

T10c12 CLA Treatment Causes Lipid Depletion and Cell Loss in RP Tissues

Fixed RP tissue sections were stained with Sytox green to visualize the nuclei (Fig. 2, *A* and *B*) and Sudan black to

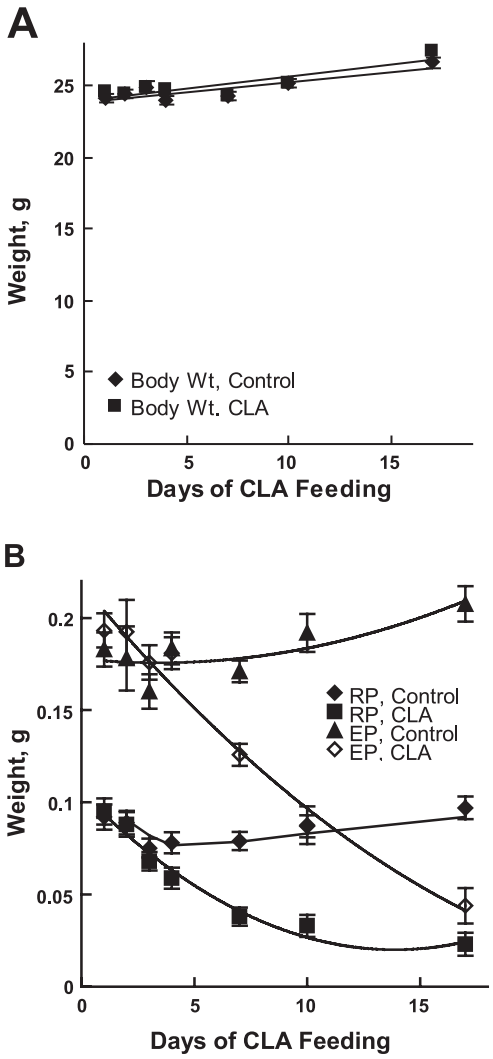

Fig. 1. Body weight changes in control (◆) and trans-10, cis-12 conjugated linoleic acid (CLA)-fed mice (■) (*A*) and weight changes of retroperitoneal (RP) adipose tissue of control (◆) and CLA-fed mice (■) and in epididymal (EP) control (▲) and CLA-fed mice(◇) (*B*). The error bars delineate SE.

visualize the adipocytes (data not shown). We found nuclear densities of 1.5 and 5.7 nuclei per 353 μm^3 for the control (n = 6 mice, 24 images) and t10c12 CLA-treated tissues (n = 6 mice, 18 images), respectively. The average weights of the control (n = 6) and t10c12 CLA-treated RP tissues (n = 6) were 157 and 23 mg, respectively. The almost fourfold increase in cell density is offset by the 6.8-fold reduction in tissue weight such that the t10c12 CLA-treated RP tissues contained only 53% of the number of total cells in the control tissue due to the much smaller mass of the t10c12 CLA-treated tissue.

H&E-stained sections were used for quantitative measurement of the cell diameters of the adipocytes. The average diameter of the adipocytes (measured from 63 frames of images from 6 mice from each group) was reduced from 46 μm for the control to 17 μm for the t10c12 CLA-treated cells. This corresponds to a 95% reduction in cell volume. The reduced adipocyte cell sizes caused the t10c12 CLA-treated WAT to have a higher density of nonadipocyte cell types (Fig. 2, *C* and *D*). The majority of the adipocytes were retained in the WAT as the ratio of the number of adipocytes in the t10c12 CLA-treated to control tissues was determined to be 0.85. The apparent 15% reduction in the number of adipocytes could be due to either cell death or a change in the adipocytes' appearance due to loss of the distinguishing lipid droplet.

T10c12 CLA Treatment Increases the Density of Macrophages in RP Tissues

T10c12 CLA treatment induces a strong inflammatory response as described below in the microarray results. The involvement of macrophages in this process was examined by confocal immunofluorescence microscopy. We counted the monocytes/macrophages containing CD68 antigen in 50 images each for the control and t10c12 CLA-treated adipose tissues. Most control tissue sections lacked macrophages although some images contained one or two macrophages (Fig. 2*E*). Macrophages were more abundant in t10c12 CLA-treated tissues, and in some cases six or seven macrophages were found in the same image (Fig. 2*F*). Additionally the t10c12 CLA-treated samples contained more monocytes in blood vessels (Fig. 2*G*) than in control sections (data not shown). We counted 6.5 times more CD68-labeled cells in the t10c12 CLA-treated samples compared with the controls. The t10c12 CLA-treated RP tissue weighed 6.8 times less than control tissue, indicating both tissues contained similar numbers of macrophages despite their much higher density in the t10c12 CLA-treated WAT. The number of macrophages was calculated from the tissue images to be 4% of the cells in control tissues and 8% of the cells in t10c12 CLA-treated tissues, which had lost 47% of their total cells as described above.

The above histological interpretation is supported by an increase in the expression of genes specific for macrophages (Supplemental Table 7). The microarray data show six- and threefold increases in CD68 (20) and F4/80 (28), respectively, as early as 2 days after t10c12 CLA feeding and persisting at ~10-fold for the duration of the experiment. Similar increases are seen for macrophage scavenger receptor 1 (14) and CCL2 [monocyte chemoattractant protein (MCP)-2, see Ref. 26], and these increase by 1 day after initiating t10c12 CLA feeding (Supplemental Table 7). The increases in the mRNA levels of these genes is larger than the estimated twofold increase in the percentage of macrophage cells, presumably due to increased expression levels of these mRNAs in activated macrophages.

Microarray Analysis of t10c12 CLA-Induced RP Transcriptome Changes

The analysis of the GeneChip Mouse Genome 420 2.0 microarrays showed thousands of transcripts are differentially expressed as early as the first time point at 24 h after feeding mice t10c12 CLA, and most of these transcripts maintained these changes for the duration of the 17-day experiment (Table 1). These large-scale changes in gene expression are consistent with the large-scale remodeling of the RP tissue that occurs over the treatment period. The significant changes observed for mRNAs from genes in known signaling pathways and the putative role of these pathways are shown (Table 2). Similarly, the significant changes in Kyoto Encyclopedia of Genes and Genomes-annotated metabolic pathways are shown (Table 3). Transcript levels from genes in individual metabolic pathways tended to increase or decrease as a group, and the majority of

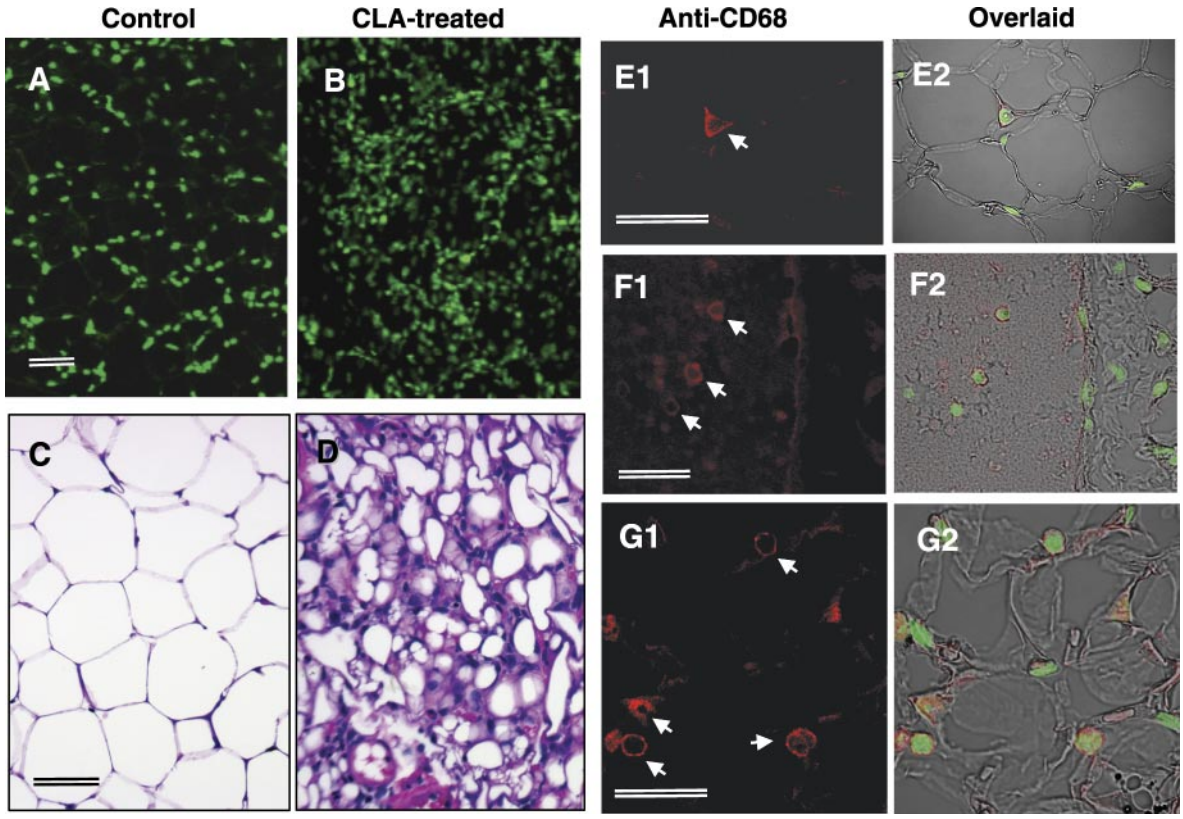

Fig. 2. Representative images showing differences in nuclear density (*A* and *B*), a comparison of adipose tissue histology (*C* and *D*), and the distribution of monocytes/macrophage as detected with antibody to CD68 (*E1*, *F1*, and *G1*; as indicated by arrows) and when overlaid with a nuclear stain (*E2*, *F2*, and *G2*) between the control and CLA-treated RP tissues. The significant increase in cell density in response to CLA, as indicated by green fluorescence-labeled nuclei (*A* and *B*), is due to both reduction of fat content and increase in number of nonadipocytes as shown in *D*. Among the nonadipocyte cells, the density of macrophages was significantly higher in the CLA-treated RP tissues (*F*) compared with that in control RP tissue sections (*E*). In addition, increased numbers of monocytes were also found in blood vessels in the CLA-treated RP tissues (*G*). Scale bars = 30 μm (*A* and *B* have the same magnification, as do *C* and *D*).

the pathways showed decreases in the transcript levels (Tables 2 and 3). As will be presented below, the directional changes in gene expression are generally conserved across multiple time points, indicating the induction or repression of individual genes are consistent over these time periods.

Lipid biosynthetic pathways. The majority of the genes in lipid biosynthetic pathways show decreased mRNA levels. These include the fatty acid biosynthesis pathways, pentose phosphate pathway, citrate cycle, oxidative phosphorylation, propanoate, butanoate, and other pathways feeding acetyl-CoA or other components necessary for fatty acid and triglyceride biosynthesis (Table 3). Rate-limiting enzymes showing strongly reduced mRNA levels include those for ATP citrate lyase and acetyl Co-A carboxylase-α and -β (Table 4). Other pathways associated with sterol biosynthesis and mitochondrial function were predominantly downregulated, including pathways associated with leucine, valine, and isoleucine degradation, ubiquinone biosynthesis, and several pathways involves with amino acid metabolism (Table 3).

Table 1. *Change in mRNA levels in RP tissues of CLA-fed mice*

Days of Feeding	Number of mRNAs That Change		
	Total Increased or Decreased	Increased	Decreased
1	5407 (2682)	2530 (1212)	2877 (1470)
2	6755 (3108)	3633 (1792)	3122 (1316)
3	8750 (3955)	4330 (2068)	4420 (1887)
4	9097 (4216)	4773 (2385)	4324 (1831)
7	7766 (3290)	3969 (1905)	3797 (1385)
10	8107 (3388)	4130 (1915)	3977 (1473)
17	7270 (3495)	3902 (2111)	3368 (1384)

An mRNA level was considered differentially increased or decreased if the false discovery rate-adjusted *P* value was <0.05. Numbers in parentheses represent values with at least a 2-fold signal change ($P < 0.01$). RP, retroperitoneal; CLA, conjugated linoleic acid.

Lipolysis. Downregulation of transcripts for the key lipolytic enzymes involved in transport of fatty acids out of the adipocytes included those for hormone sensitive lipase, adiponutrin, desnutrin, and monoglyceride lipase (Table 4). Monoglyceride lipase is normally highly expressed as its transcript levels are more abundant than 99% of the mRNA signals. Hormone-sensitive lipase is also highly expressed as it is in the top 95th percentile. Even after two- to sevenfold declines, their mRNA levels are still in the 90th percentile of the most abundant mRNA signals suggesting that some residual lipase activity may still be present in this pathway. The 25–40% downregulation of lipoprotein lipase would be consistent with a decline in lipid filling capacity. In contrast there is a significant upregulation of lipase A, the lysosomal acid lipase (also known as cholesterol ester hydrolase). This transcript is among the top 10% of the most abundant transcripts in the controls and rises

Table 2. *mRNA changes in canonical signaling pathways in RP tissues of CLA-fed mice*

Canonical Signaling Pathways	Interpretive Biological Role	Days after CLA Feeding: 1	2	3	4	7	10	17	mRNA Change Summary
		Number of mRNAs Changed							
PPAR signaling (65)	adipocyte dedifferentiation possibly due to inflammation factors and NF-κB signaling	27*	17	22	25	18	22	20	mixed
Chemokine signaling (56)	inflammation responses of adipocytes, macrophages and other cells	26*	23	31*	34*	28*	28*	26*	mostly up
PI3K/AKT signaling (88)	activation of IL-6, insulin-receptor signaling	35*	34*	44*	43*	38	37	35	mixed
ERK/MAPK (121)	activation of IL-6, insulin-receptor signaling, IL-4, IL-2 signaling	45*	56*	65*	55*	55*	55*	52*	mixed
B-cell receptor signaling (114)	immune cell activation and infiltration	41*	47*	57*	59*	50*	51*	49*	mostly up
IL-6 signaling (68)	inflammatory responses	26*	21	28	27	27	22	21	mostly up
IL-2 signaling (40)	inflammatory responses	15	14	19	21	21*	21*	19*	mixed
IL-4 signaling (36)	inflammatory responses	14	12	19	21*	23*	22*	21*	mostly up
JAK/Stat signaling (47)	inflammatory responses	19*	16	27*	27*	26*	27*	25*	mixed
Insulin receptor signaling (102)	insulin resistance	36*	36	49*	46	45	43*	43*	mixed
IGF-1 signaling	antiproliferation	24	26	33*	35*	33*	32*	29*	mixed
VEGF signaling (66)	antiproliferation of vasculature	25	27	34*	36*	35	39*	29	mixed
Cell cycle: G2/M DNA damage checkpoint signaling (34)	antiproliferation, potentiates apoptosis or DNA repair	7	16	18	21*	17*	18*	17*	mostly up
Apoptosis signaling (68)	potentiates associated with deproliferation	31*	27	34*	35*	28	26	25	mixed
Integrin signaling (164)	antimitotic/proliferation, cell cycle regulation	39	51	68	72	69*	68	61	mixed
Sonic hedgehog signaling (22)	antiproliferation of vasculature	8	8	13*	13*	11	10	10	mixed
Nitric oxide signaling in the cardiovascular system (41)	insulin resistance, anti-proliferation of vasculature	17*	17	26*	26*	21	16	16	mixed

Listed under Canonical Signaling Pathways are the conceptual signaling pathways with the total number of genes in the Kyoto Encyclopedia of Genes and Genomes (KEGG)-derived pathways listed in parenthesis. *Gene groups where *P* value is ≤0.05.

to an even higher level in t10c12 CLA-fed mice. The increased transcript abundance of this gene may be associated with phagocytotic immune cells and vascular cells rather than adipocytes.

Apoptosis. Pathway analysis indicated that a number of genes involved in apoptotic signaling were differentially expressed (Table 2 and Supplemental Table 5). There is an induction of a number of death receptors and their ligands

Table 3. *mRNA changes in metabolic signaling pathways in RP tissues of CLA-fed mice*

Metabolic Pathway (number of genes in pathway)	Days after CLA Feeding: 1	2	3	4	7	10	17	mRNA Change Summary
	Number of mRNAs Changed							
Leucine, valine and isoleucine degradation (58)	42*	45*	48*	45*	37*	40*	39*	all decreased
Propanoate metabolism (57)	36*	39*	44*	42*	36*	35*	35*	all decreased
Citrate cycle (27)	21*	23*	21*	20*	14*	14*	14*	all decreased
Oxidative phosphorylation (139)	67*	76*	81*	64	41	39	35	most decreased
Ubiquinone biosynthesis (47)	28	30*	33	23	13	12	9	all decreased
Fatty acid biosynthesis (path 1, 18)	14*	14*	14*	13*	9	13*	13*	all decreased
B-alanine biosynthesis (49)	24*	29*	31*	30*	25*	26*	24*	most decreased
Butanoate metabolism (44)	23*	25*	26*	25*	24*	25*	21*	all decreased
Fatty acid biosynthesis (path 2, 8)	7*	6*	6*	7*	7*	6*	6*	all decreased
Alanine and aspartate metabolism (28)	15*	13	15	17*	16*	15*	13	most decreased
Pyruvate metabolism (69)	30*	35*	44*	41*	38*	34*	34*	all decreased
Cysteine metabolism (12)	8*	8*	8*	7	6	6	6	mixed
Glutathione metabolism (61)	26*	31*	31*	28	24	27	25	most decreased
Glutamate metabolism (34)	16*	17*	17	19*	18*	15	13	mixed
Lysine metabolism (46)	20*	25*	29*	29*	24*	23*	22*	most decreased
Histidine metabolism (32)	15*	18*	18*	19*	17*	16*	15*	most decreased
Pantheonate metabolism (19)	10*	9	11	12*	9	10	9	mixed
One carbon by folate metabolism (19)	10*	9	12*	13*	13*	13*	12*	mixed
Fatty acid metabolism (111)	41*	44*	50*	49*	43*	46*	49*	most decreased
Riboflavin metabolism (17)	9*	9	11*	9	9	9	9	most decreased
Synthesis and degradation of ketone bodies (10)	6*	4	4	3	4	4	3	all decreased
Glycerolipid metabolism (79)	27	30	37*	39*	36*	33	33	mixed
Tyrosine metabolism (45)	16	18	22	23	20	22*	22*	mixed
Aminosugar metabolism (25)	9	15*	17*	17*	15*	14*	14*	most increased

Listed are the conceptual signaling pathways with the total number of genes in the KEGG-derived pathways listed in parenthesis. *Gene groups where *P* value is ≤0.05.

Table 4. *mRNA changes in key genes in fatty acid and lipid biosynthesis in RP tissues of CLA-fed mice*

Gene Symbol	Description	Days of *trans*-10 *cis*-12 CLA Feeding						
		1	2	3	4	7	10	17
	Fatty Acid, Glucose, or Lipid Transport	mRNA Changes (fold-change; control = 1.0)						
ABCD2	ATP-binding cassette, sub-family D (ALD), member 2	0.2	0.4	0.2	0.2	0.3	0.2	0.2
SLC2A4	facilitated glucose transporter member 4, Glut 4	0.2	0.1	0.1	0.1	0.3	0.2	0.2
SLC2A5	facilitated glucose/fructose transporter member 5	0.3	0.2	0.1	0.2	0.2	0.3	0.2
FABP4	fatty acid binding protein 4, adipocyte, aP2	0.4	0.4	0.2	0.4	0.3	0.3	0.2
LRP8	low density lipoprotein receptor-related protein 8	9.2	3.2	3.2	2.8	n.c.	n.c.	n.c.
CAV1	caveolin 1	0.6	n.c.	0.8	0.7	0.6	0.6	0.6
CAV2	caveolin 2	0.6	0.7	0.6	0.6	0.5	0.5	0.5
MSR1	macrophage scavenger receptor 1	8.0	21.1	12.1	10.6	7.5	6.5	11.3
	Lipolysis							
ADPN	adiponutrin	0.2	0.3	0.2	0.1	0.1	0.1	0.1
LIPE	lipase, hormone-sensitive	0.2	0.3	0.2	0.3	0.3	0.2	0.1
LIPA	lipase A, lysosomal acid, cholesterol esterase	2.0	9.2	17.1	11.3	9.8	9.8	8.6
MGLL	monoglyceride lipase	0.2	0.4	0.3	0.3	0.3	0.3	0.3
LPL	lipoprotein lipase	0.6	0.7	n.c.	n.c.	0.7	0.8	0.8
PNPLA2	datatin-like phospholipase domain containing 2,	0.6	0.3	0.3	0.3	0.4	0.3	0.3
	Lipogenesis, fatty acid biosynthesis and metabolism							
ACACA	acetyl-coenzyme A carboxylase alpha	0.3	0.2	0.1	0.2	0.2	0.2	0.2
ACACB	acetyl-coenzyme A carboxylase beta	0.4	0.2	0.2	0.3	0.2	0.2	0.1
ACAD8	acyl-coenzyme A dehydrogenase family, member 8	0.5	0.4	0.5	0.4	0.5	0.4	0.6
ACSL1	acyl-coA synthetase long-chain family member 1	0.3	n.c.	0.5	0.6	0.7	0.6	0.7
ACAS2	acetyl-coenzyme A synthetase 2	0.4	0.2	0.3	0.3	0.2	0.1	0.1
ACAT1	acetyl-coenzyme A acetyltransferase 1	0.4	0.4	0.4	0.3	0.5	0.4	0.5
ACAT2	acetyl-coenzyme A acetyltransferase 2	0.3	0.3	0.2	0.4	0.3	0.2	0.2
ACLY	ATP citrate lyase	0.2	0.2	0.1	0.2	0.2	0.2	0.1
ACO1	aconitase 1, soluble	0.4	0.5	0.5	0.4	0.4	0.4	0.5
ACSL1	acyl-CoA synthetase long-chain family member 1	0.3	n.c.	0.5	0.6	0.7	0.6	0.7
AGPAT2	1-acylglycerol-3-phosphate O-acyltransferase 2	0.2	0.5	0.4	0.5	0.5	0.4	0.4
CS	citrate synthase	0.6	0.4	0.5	0.6	0.7	0.8	0.7
DF	D component of complement (adipsin)	0.6	0.4	0.4	0.4	0.2	0.2	0.1
EHHADH	enoyl-Co A, hydratase/3-hydroxyacyl coenzyme A	0.3	0.3	0.2	0.3	0.4	0.4	0.3
ELOVL6	ELOVL family member 6, elongation of long chain fatty	0.2	0.1	0.1	0.1	0.1	0.1	0.1
FABP4	fatty acid binding protein 4, adipocyte	0.4	0.4	0.2	0.4	0.3	0.3	0.2
FASN	fatty acid synthase	0.5	0.3	0.3	0.3	0.3	0.3	0.3
GPD2	glycerol-3-phosphate dehydrogenase 2 (mitochondrial)	0.2	0.1	0.1	0.1	0.3	0.3	0.2
HADH2	hydroxyacyl-coenzyme A dehydrogenase, type II	0.4	0.4	0.4	0.4	0.5	0.4	0.6
IDH3A	isocitrate dehydrogenase 3 (NAD+) alpha	0.4	0.4	0.5	0.4	n.c.	n.c.	n.c.
LSS	lanosterol synthase	0.3	0.5	0.4	0.5	0.8	0.6	0.6
MCCC2	methylcrotonoyl-coenzyme A carboxylase 2 (beta)	0.2	0.2	0.1	0.2	0.7	0.6	0.7
ME1	malic enzyme 1, NADP(+)-dependent, cytosolic	0.6	0.3	0.4	0.5	0.2	0.2	0.3
MGLL	monoglyceride lipase	0.2	0.4	0.3	0.3	0.3	0.2	0.3
PC	pyruvate carboxylase	0.4	0.1	0.2	0.2	0.3	0.3	0.3
PCK1	phosphoenolpyruvate carboxykinase 1 (soluble)	0.1	0.1	0.0	0.1	0.6	0.4	0.5
PDHA1	pyruvate dehydrogenase (lipoamide) alpha 1	0.5	0.3	0.3	0.4	0.4	0.4	0.3
PDK1	pyruvate dehydrogenase kinase, isoenzyme 1	0.2	0.2	0.2	0.3	0.5	0.4	0.4
SC5DL	sterol-C5-desaturase	0.3	0.4	0.3	0.3	0.4	0.4	0.4
SCD	stearoyl-CoA desaturase (delta-9-desaturase)	0.4	0.2	0.3	0.4	0.5	0.5	0.5
SCD2	stearoyl-coenzyme A desaturase 2	0.1	0.3	0.1	0.6	0.3	0.3	0.2
	Beta Oxidation Genes							
CPT1A	carnitine palmitoyltransferase 1A (liver)	n.c.	2.6	2.1	3.0	2.3	2.3	2.1
CPT1B	carnitine palmitoyltransferase 1B (muscle)	n.c.	n.c.	n.c.	n.c.	3.0	3.2	1.6
CROT	carnitine O-octanoyltransferase	0.5	0.7	0.7	0.7	n.c.	n.c.	n.c.
CPT2	carnitine palmitoyltransferase II	0.5	0.4	0.6	0.5	0.7	0.6	0.6
ECHS1	enoyl coenzyme A hydratase, short chain, 1,	0.4	0.2	0.3	0.4	0.6	0.5	0.4
CRAT	carnitine acetyltransferase	0.3	0.3	0.3	0.4	n.c.	0.4	0.5
NDUFC2	NADH dehydrogenase (ubiquinone) 1, subcomplex	0.5	0.7	0.7	n.c.	n.c.	n.c.	n.c.
NDUFV2	NADH dehydrogenase (ubiquinone) flavoprotein 2Da	0.7	0.7	0.7	n.c.	n.c.	n.c.	n.c.
ACADM	acyl-coenzyme A dehydrogenase, C-4 to C-12 straight	0.4	0.5	0.7	0.7	n.c.	n.c.	n.c.
HADHSC	L-3-hydroxyacyl-coenzyme A dehydrogenase, short	0.6	0.5	0.5	0.5	0.8	0.6	0.6
AUH	AU RNA binding protein/enoyl-coenzyme A hydratase	0.5	0.4	0.4	0.4	0.4	0.4	0.4
HADHB	hydroxyacyl-coenzyme A dehydrogenase/3-ketoacyl-	0.5	0.5	0.6	n.c.	n.c.	n.c.	n.c.
ACADVL	acyl-coenzyme A dehydrogenase, very long chain	0.8	0.5	0.5	0.7	n.c.	n.c.	n.c.
ACADSB	acyl-coenzyme A dehydrogenase, short/branched chain	0.7	0.3	0.4	0.3	0.4	0.4	0.4
ACADL	acyl-coenzyme A dehydrogenase, long chain	0.6	0.5	0.7	0.8	n.c.	n.c.	n.c.
ACAD9	acyl-coenzyme A dehydrogenase family, member 9	0.5	n.c.	0.7	0.7	0.8	0.7	0.8
ACADL	acyl-coenzyme A dehydrogenase, long chain	0.6	0.5	0.7	0.8	n.c.	n.c.	0.4

n.c., no change.

Table 5. *Quantitative RT-PCR verification of selected mRNA signal changes*

Gene Description	Gene Symbol	Days of *trans*-10 *cis*-12 Linoleic Acid Feeding				
		1	2	3	4	7
		Average Relative Expression Value ± SE (n = 3)				
Lipin 1-α	LPIN1-α	1.50 ± 0.2	0.55 ± 0.1	0.51 ± 0.1	0.85 ± 0.1	0.78 ± 0.1
Lipin 1-β	LPIN1-β	0.36 ± 0.0	0.43 ± 0.1	0.53 ± 0.1	0.21 ± 0.0	0.21 ± 0.0
CCAAT/enhancer binding protein-α	CEBPA	0.38 ± 0.1	0.48 ± 0.1	0.37 ± 0.0	0.16 ± 0.1	0.59 ± 0.1
Peroxisome proliferative activated receptor-γ	PPARG	0.14 ± 0.0	0.57 ± 0.	0.28 ± 0.0	0.18 ± 0.0	0.38 ± 0.0
Fatty acid binding protein 4, AP-2	FABP-4	0.44 ± 0.0	0.10 ± 0.0	0.47 ± 0.1	0.47 ± 0.1	0.57 ± 0.1
Preadipocyte factor-1 PREF-1	DLK-1	1.50 ± 0.2	0.44 ± 0.1	0.48 ± 0.1	0.43 ± 0.1	0.57 ± 0.1

The average relative expression values shown are the expression values relative to the control mRNA of β2 microglobulin.

including TNF superfamily members, TNF ligands, and TNF-responsive genes. The p53 mRNA levels did not change, but there was a strong increase in MdM-2 mRNA, which is induced in response to p53 to foster clearance (19). The proapoptotic genes APAF1, BAX, PMAIP1, and MCL1 were moderately upregulated. Two cell death-inducing DDFA-like effectors were strongly downregulated (CIDEA, CIDEC), and others moderately but consistently downregulated are: CARD6, CARD10, FAS, BCL2L13, BNIP3, cytochrome c, and AATK. There were strong increases in the genes involved in DNA repair, PCNA and GADD45B, and also the cell cycle arrest-associated mRNAs, CDKNA1 (pRB). Retinoblastoma nuclear protein genes individually changed consistently over time, but the transcript levels for some family members increased while the levels decreased for others. The antiapoptotic genes BCL2, BCL2-W, BAG1, and BAG4 declined in abundance. However, the antiapoptotic genes, such as BCL2L11 (BCL2-XL), BCL2A1, BAG2, and the IAP-related survival genes, including NAIP, c-IAP1, BIRC4, and survivin were strongly upregulated (Table 2, Supplemental Table 6). There were increases in the proinflammatory initiator caspases 1 and 4, but relatively little induction of the other caspases. The mixture of transcript changes may reflect the different cell types and fates in the WAT. Overall the changes at the transcriptional level seem to favor cell cycle arrest and survival rather than apoptosis.

Energy expenditure. One mechanism for lipid depletion that has been proposed is an increase in energy expenditure via an increase in thermogenic energy via UCPs. UCP1 and UCP2 transcript levels increased 26- and 4-fold, at abundance levels that places them in the 95th and 90th percentiles in probe set signal strengths, respectively, These values agree with the 33- and 8-fold changes observed for UCP-1 and -2, respectively, in the quantitative RT-PCR (QRT-PCR) analysis (Tables 5 and 6). These increases occurred 3–7 days after t10c12 CLA treatment initiation, which is about when the most rapid fat loss occurs (Fig. 1). Additionally, carnitine palmitoyltransferase 1 (CPT1) mRNA levels were increased (Table 4). The combination of increased transcript levels for UCP1 and CPT1 suggests increased fatty acid oxidation is occurring.

Adipocyte transcription factors. Key transcription factors regulating adipocyte differentiation and gene expression had reduced expression levels as early as 24 h after t10c12 CLA treatment. These include PPAR-γ, CAAT/enhancer binding protein (C/EBP)-α, retinoic acid receptor-x, and SREBP1 (Table 7). There was also a transient downregulation on *day 1* of other transcriptional factors such as PPAR-γ coactivator 1α and β (Table 7). The changes in the transcripts for PPAR-γ and C/EBP-α were confirmed by QRT-PCR (Tables 5 and 6) as were changes for preadipocyte factor-1 (Pref-1) and fatty acid binding protein. The reduced expression of the transcription factors that regulate the development and maintenance of

Table 6. *Changes in relative and absolute signal values for uncoupling proteins in RP tissues*

Gene Symbol	Gene Description	Days of trans-10 cis-12 CLA Feeding						
		1	2	3	4	7	10	17
		Microarray Fold Change in mRNA Levels						
UCP1	uncoupling protein 1					20	26	14
UCP2	uncoupling protein 2			3.0	3.7	4.3	3.4	3.9
UCP3	uncoupling protein 3	0.3	0.2	0.2	0.3	0.2	0.2	0.2
	Probe Set ID	*Microarray Probe Set Signal Values*						
UCP1	1418192_at	44	313	157	450	10,056	9723	4114
UCP2	1448188_at	1000	2684	3808	6250	5956	5250	4926
UCP2	1459740_s_at	1138	1943	3236	4235	3784	4054	4929
UCP3	1420657_at	242	327	230	193	285	296	157
		Average Quantitative RT-PCR Relative Expression Values ± SE (n = 3)						
UCP1	uncoupling protein 1	0.17±0.2	0.9±0.3	0.6±0.3	1.3±0.5	22±1.6	33±3	11±1.6
UCP2	uncoupling protein 2	1.3±0.4	2.8±0.6	5.0±1.2	4.0±1.2	7.9±1.3	6.0±1.2	3.7±1.2

For comparative gene expression, the microarray probe set signal values for the UCP1 and UCP2 at day 7 are higher than 98 or 95 percent of the genes on the microarray, respectively.

Table 7. *A subset of changes in nuclear genes and transcription regulators detected by Affymetrix array analysis*

Gene Symbol	Gene Description	Days of CLA Feeding						
Associated With Adipocyte Differentiation and Functions		1	2	3	4	7	10	17
CEBPA	CCAAT/enhancer binding protein (C/EBP)	0.3	0.5	0.4	0.4	0.5	0.5	0.5
EIF4EBP1	eukaryotic translation initiation factor 4E binding	0.5	0.4	0.5	0.4	0.4	0.4	0.4
EIF4EBP2	eukaryotic translation initiation factor 4E binding	n.c.	n.c.	0.7	0.6	0.5	0.5	0.5
LPIN1	lipin 1	0.2	0.4	0.2	0.3	0.3	0.3	0.2
PPARGC1	peroxisome proliferative activated receptor,	0.5	0.6	0.4	0.5	n.c.	n.c.	n.c.
PPARG	peroxisome proliferative activated receptor,	0.3	0.6	0.4	0.4	0.5	0.5	0.6
PPARGC1	peroxisome proliferative activated receptor,	0.2	n.c.	n.c.	n.c.	n.c.	n.c.	n.c.
NR1H3	nuclear receptor subfamily 1, group H, member 3	0.4	n.c.	n.c.	n.c.	n.c.	n.c.	n.c.
SREBF1	sterol regulatory element binding transcription	0.2	0.4	0.3	0.3	0.4	0.3	0.3
SREBF2	sterol regulatory element binding transcription	2.8	2.8	3.0	2.1	n.c.	n.c.	n.c.
RXRG	retinoid X receptor, gamma	0.3	0.7	0.4	0.4	0.4	0.4	0.5
WBSCR14	Williams Beuren syndrome chromosome region	0.3	0.3	0.2	0.1	0.1	0.2	0.2
NRIP1	nuclear receptor interacting protein 1	0.5	0.3	0.3	0.4	0.4	0.3	0.4
NR3C1	nuclear receptor subfamily 3, group C, member 1	0.4	0.4	0.3	0.6	0.6	0.5	0.6
PPARGC1	peroxisome proliferative activated receptor,	0.2	n.c.	n.c.	n.c.	n.c.	n.c.	n.c.
NR1D1	nuclear receptor subfamily 1, group D, member 1	0.5	0.6	0.3	0.3	0.3	0.3	0.3
CEBPD	CCAAT/enhancer binding protein (C/EBP), delta	4.3	n.c.	n.c.	n.c.	n.c.	n.c.	n.c.
THRA	thyroid hormone receptor, alpha	0.4	0.4	0.5	0.4	0.5	0.5	0.8
Transcription Factors Associated With Miscellaneous Functions								
RORC	RAR-related orphan receptor C	0.4	0.2	0.2	0.2	0.3	0.2	0.2
PLAGL1	pleiomorphic adenoma gene-like 1	0.3	0.4	0.4	0.3	0.4	0.5	0.8
ATF3	activating transcription factor 3	16.0	6.1	11.3	17.1	27.9	26.0	26.0
ATF4	activating transcription factor 4	7.0	4.3	5.3	4.3	3.0	3.0	4.3
MAFF	v-maf musculoaponeurotic fibrosarcoma	12.1	3.5	2.6	3.5	2.3	4.0	2.6
EGR1	early growth response 1	8.0	1.6	2.1	2.8	2.6	5.3	2.6
EGR2	early growth response 2	6.5	8.0	8.0	10.6	16.0	21.1	21.1
EGR3	early growth response 3	3.5	2.0	n.c.	2.3	3.5	6.5	4.9
EAF1	ELL associated factor 1	7.5	2.0	2.3	2.0	1.7	1.9	1.9
FOS	v-fos FBJ murine osteosarcoma viral oncogene	7.5	17.1	19.7	26.0	13.9	14.9	12.1
FOSL1	FOS-like antigen 1	21.1	3.5	7.5	10.6	2.6	4.3	2.6
FOSL2	FOS-like antigen 2	3.5	2.0	n.c.	n.c.	n.c.	1.6	1.5
DNMT3L	DNA (cytosine-5-)-methyltransferase 3-like	7.5	1.9	2.3	2.3	2.0	2.3	1.7
MYC	v-myc myelocytomatosis viral oncogene	7.5	n.c.	2.5	3.5	2.6	4.0	2.3
DDIT3	DNA-damage-inducible transcript 3	6.5	1.5	3.0	4.6	3.7	3.7	3.2
JUN	v-jun sarcoma virus 17 oncogene homolog	4.6	2.0	2.6	2.3	2.3	2.3	2.5
JUNB	jun B proto-oncogene	5.3	2.5	3.2	4.3	4.3	5.3	4.3
DSCR1	Down syndrome critical region gene 1	5.3	n.c.	1.6	1.7	1.7	1.9	1.6
RELB	v-rel reticuloendotheliosis viral oncogene	4.0	n.c.	n.c.	n.c.	1.9	1.7	2.0
TGIF	TGFB-induced factor (TALE family homeobox)	4.0	2.5	3.2	3.5	4.0	4.9	4.9
NFKBIZ	nuclear factor of kappa light polypeptide gene	4.0	2.0	n.c.	n.c.	n.c.	2.6	3.7

The values represent fold-change relative to control where control = 1.0. A full subset is available in the supplemental data set.

adipocyte physiology is consistent with the sustained reduction of the mRNA transcripts for enzymes in metabolic pathways associated with lipid and fatty acid anabolic pathways (Tables 3 and 4). For example, the PPAR-γ-modulated genes that are downregulated include key metabolic genes such as aP2, SCD, LPL ACC, FASN, and Glut4 (Table 4).

Downregulation of lipin 1 in adipose tissue. Lipin 1 transcripts were consistently downregulated two- to sevenfold by t10c12 CLA treatment at the different time points (Table 7). The lipin 1 gene (*Lpin1*) may play a role in t10c12 CLA-mediated lipid loss because a genetic mutation of the gene causes a lypodystrophy (38) with symptoms remarkably similar to the syndrome caused by t10c12 CLA feeding. Two alternatively spliced *Lpin1* variants have been characterized, lipin-α and lipin-β. The microarray probe sets either were specific for the larger lipin-β transcript or detected the mRNA portions in common between the two forms. RT-PCR primer sets that distinguish these two forms (37) were used both to confirm the microarray expression results and to better distinguish the two types of mRNAs by QRT-PCR of mRNA from control and t10c12 CLA-treated RP tissues (Table 5). There was a transient increase in the relative mRNA abundance for lipin-α on *day 1* and modest reductions in expression thereafter. The significant differential downregulation of lipin-β was confirmed (Table 5). The relative abundances of the two alternatively spliced *Lpin1* mRNAs were determined by performing endpoint RT-PCR using two primers that produce different size products for the lipin-α and lipin-β mRNA forms. The lipin-β mRNA form was found to be the major form of *Lpin1* mRNA in the adipose tissues (Supplemental Fig. 3). This is in contrast to the higher relative ratio of the lipin-α form in 3T3L1 mRNAs (Ref. 37 and Supplemental Fig. 3). The significant reduction of the much more abundant lipin-β mRNA is consistent with the microarray results, as the more modest changes in the lipin-α mRNA would not contribute to detectable differences on the microarray probe set that detects the combined amounts of both of the *Lpin1* mRNAs splice isoforms.

Table 8. *A subset of mRNA changes in genes of characterized and putative adipocytokines and associated inflammation detected by Affymetrix array analysis*

Gene Symbol	Gene Description	Days of CLA Feeding						
		1	2	3	4	7	10	17
DF	D component of complement (adipsin)	0.6	0.4	0.4	0.4	0.2	0.2	0.1
ADIPOQ	adiponectin	0.5	0.4	0.5	0.5	0.5	0.5	0.6
ADIPOR2	adiponectin receptor 2	0.4	0.6	0.3	0.4	0.4	0.4	0.4
PBEF1	visfatin	n.c.	0.5	0.4	0.5	n.c.	n.c.	n.c.
LEP	leptin	0.2	n.c.	0.5	0.3	0.2	0.1	0.2
RETN	resistin	0.6	0.3	0.3	0.4	0.3	0.3	0.3
RBP4	retinol binding protein 4, plasma	0.5	0.2	0.3	0.2	0.2	0.1	0.2
VEGF	vascular endothelial growth factor	0.6	0.3	0.4	0.3	0.3	0.4	0.4
VEGFB	vascular endothelial growth factor B	0.3	0.2	0.2	0.2	0.2	0.2	0.2
SERPINE1	serine proteinase inhibitor, PAI-1	55.7	12.1	14.9	5.3	5.7	9.2	7.5
TNF	tumor necrosis factor	1.6	n.c.	1.6	1.5	n.c.	n.c.	n.c.
IL6	interleukin 6 (interferon, beta 2)	18.4	1.7	n.c.	n.c.	n.c.	n.c.	n.c.
IL1B	interleukin 1, beta	6.5	1.7	1.9	n.c.	n.c.	1.5	1.4
CASP1	caspase 1, apoptosis-related (interleukin 1, beta, convertase)	1.6	2.3	2.5	3.2	4.6	4.3	4.6
CASP4	caspase-4, Interleukin 1 beta convertase homolog, ICH2	8.0	2.5	2.8	3.2	3.0	3.5	4.0
IL1RN	interleukin 1 receptor antagonist	4.0	18.4	27.9	73.5	32.0	17.1	7.5
PTX3	pentraxin-related gene, IL-*tB* induced	78.8	7.5	24.3	36.8	11.3	21.1	21.1
IKBKB	inhibitor of kappa light polypeptide gene enhancer in B-cells, kinase beta (IKK-beta)	1.5	1.5	2.0	1.4	n.c.	n.c.	n.c.
IKBKE	inhibitor of kappa light polypeptide gene enhancer in B-cells, kinase epsilon (IKK epsilon)	1.9	3.5	4.6	7.0	5.3	5.7	4.6
IL10	interleukin 10	n.c.	3.5	4.6	4.3	2.3	2.1	n.c.
NOS3	nitric oxide synthase 3 (endothelial cell)	0.3	0.2	0.2	0.2	0.2	0.1	0.1
NOSTRIN	nitric oxide synthase trafficker	n.c.	3.0	4.3	4.3	4.3	4.9	4.9
IL15	interleukin 15	n.c.	n.c.	2.1	1.7	6.1	6.5	10.6
PTGS2	prostaglandin-endoperoxide synthase 2 (Cox-2)	2.1	n.c.	n.c.	n.c.	1.4	1.4	1.4
PTGER2	prostaglandin E receptor 2 (subtype EP2), 53kDa	n.c.	3.0	2.6	4.6	5.3	4.3	5.3
PTGER3	prostaglandin E receptor 3 (subtype EP3)	0.2	0.4	0.3	0.3	0.2	0.2	0.2
PTGER4	prostaglandin E receptor 4 (subtype EP4)	4.0	3.0	3.5	2.8	2.3	2.8	3.7
PTGES	prostaglandin E synthase	0.4	0.3	0.2	0.3	0.2	0.2	0.2
PTGER3	prostaglandin E receptor 3 (subtype EP3)	0.2	0.4	0.3	0.3	0.2	0.2	0.2
PTGER4	prostaglandin E receptor 4 (subtype EP4)	4.0	3.0	3.5	2.8	2.3	2.8	3.7
SPP1	secreted phosphoprotein 1	4.6	119.4	84.4	147.0	9.8	21.1	22.6
ADFP	adipose differentiation-related protein	1.4	1.7	1.5	2.3	1.6	1.4	n.c.
S100A9	S100 calcium binding protein A9	11.3	8.0	n.c.	n.c.	n.c.	n.c.	n.c.
ANGPT2	angiopoietin 2	n.c.	1.5	3.7	4.3	2.8	2.8	2.8
NGFB	nerve growth factor, beta	4.9	3.7	1.9	3.5	n.c.	n.c.	n.c.
SAA3	serum amyloid A 3	4.3	8.0	4.3	3.7	3.7	3.5	3.2
LGALS3	lectin, galactoside-binding, soluble, 3	13.0	22.6	27.9	32.0	27.9	21.1	16.0
THBS1	thrombospondin 1	12.1	2.6	3.5	2.6	2.5	7.0	3.7
HSPA1B	heat shock 70-kDa protein 1B	73.5	4.3	8.0	3.5	2.5	3.2	3.5
HSPA1A	heat shock 70-kDa protein 1A	55.7	3.0	5.3	3.0	1.9	2.6	3.0
TIMP1	tissue inhibitor of metalloproteinase 1	9.8	42.2	8.6	12.1	5.7	11.3	8.0
GLIPR1	GLI pathogenesis-related 1 (glioma)	3.7	11.3	12.1	18.4	34.3	32.0	45.3
TIMP1	tissue inhibitor of metalloproteinase 1	9.8	42.2	8.6	12.1	5.7	11.3	8.0
CSF1	colony stimulating factor 1	6.1	2.6	1.6	n.c.	n.c.	1.9	2.0
CXCL or CCL*								

The values represent fold-change relative to control where control = 1.0. *CXCL ot CCL motif genes > 28 genes, 2- to 30-fold induction, see supplemental data.

Chemokines and inflammation. IL-6 increased within a 24-h period, was slightly elevated at 48 h, and subsided at later time points. Sustained increases in the levels of the mRNAs of TNF-α-responsive receptors and responsive genes were found over the longer term (Table 8). Increases in mRNAs of IL1B, IL10, IL15, IL17, and in the receptors IL1RN, IRAKB, ILR1, IL10R; IL10RA, IL10RB, IL17R, IL13R, IL13RA, and IL2RT were also observed. The mRNA levels for the NFKB family of related proteins NFKBIA, NFKBIB, NFKBIE, and NFKIBIZ also increased.

Extracellular factors (CCL7 or MCP-7) CCL4 or MPlB are increased as are other cytokines and cytokine receptors. At least 28 CXCL or CCL motif genes were strongly induced (2- to 30-fold) in the RP tissue as a result of t10c12 CLA feeding. An examination of the signaling pathways impacted (Table 2) shows 8 of the 20 pathways listed are directly involved in inflammation, including IL-6, IL-2, IL-4, JAK/STAT, Beta cell receptor, chemokine, ERK/MAPK, and phosphatidylinositol 3-kinase/AKT signaling. Finally, a high proportion of the transcription factors with relatively strong signal increases is known to be associated with responses to inflammation and TNF-α or NF-κB modulation (Supplemental Tables 2 and 5), strengthening the conclusion of a strong inflammatory response.

DISCUSSION

A range of feed intake responses have been found in mice, for a number of different genotypes, that were fed mixed or pure isomers of CLA. These reports generally agree that differences in feed intake, when observed, do not account for CLA-induced WAT weight loss (17, 22, 36). For example, AKR/J male mice fed a diet containing 1% of mixed isomers of CLA, containing 41% of the t10c12 CLA isomer, showed no reduction in feed intake or body weight relative to control mice after 2 wk of feeding while maintaining a 40% reduction in RP WAT mass (10). In a prior study from the same group, a suppression of feed intake was observed that was later interpreted to be possibly due to feed aversion resulting from simultaneous changes in diet and CLA treatment (10). Reductions in feed intake (11%) and total body weight were observed with MC colony mice fed a diet containing a 0.5% CLA as a mixture of c9t11 and t10c12 isomers with a concurrent loss of 49–70% of the mass of the RP WAT (18). However, a second study under the same conditions with ML or MH colony mice showed no reduction in feed intake or body weight while still showing similar reductions in body fat (18). The range of WAT weight losses reported in different studies may be due to diet-genotype interactions, but this has not been conclusively demonstrated. We found no reduction in feed intake or body weight in our study, facilitating the assignment of the 75% or more reduction in RP WAT weight to the metabolic effects of consuming dietary t10c12 CLA.

A common and surprising finding in many CLA-feeding experiments is that the total body weights of control and treated animals are often similar despite the reduced fat content of the CLA-fed mice. This can be explained in part by the increase in liver and spleen size in some experiments (10, 18, 50) and the reduced caloric content of the carcasses of the CLA-fed animals (48). In this latter study BALB/c male mice were fed mixed CLA isomers containing 0.45% t10c12 CLA for 39 days. The body weights of the CLA-fed mice were 96% of the controls, but the energy content of these mice was only 63% of the control mice due to a decrease in fat content and increase in water content (48).

A recent study of the transcriptome response of obese mice fed 1% t10c12 CLA for 5 or 14 days found a 30% weight loss in epididymal adipose tissues and evidence of expression changes for genes involved with apoptosis, energy expenditure, fatty acid oxidation, lipolysis, inflammation, lipogenesis, and blockage of preadipocyte differentiation (21). The number of gene expression changes was relatively small with only 29 and 125 genes altered twofold or more ($P < 0.01$) after 5 and 14 days, respectively (21). Our experiments with RP adipose tissues found between 2,682 and 4,216 genes changed expression levels by at least twofold ($P < 0.01$, Table 1). The classes of transcript changes generally agree with those found in the earlier study (21) and considerably expand the description of genes that respond to t10c12 CLA. This larger number of detected changes resulted from the recent availability of the Affymetrix GeneChip Mouse Genome 420 2.0 microarray that surveys over 34,000 mRNA transcripts.

Apoptosis

Our histological data indicate the major mechanism of delipidation is not mediated by apoptosis. We found at least 85% of the number of adipocytes in the control WAT are still present in the WAT under conditions where the treated tissue has lost 75% or more of its mass. This is consistent with results from our and other studies showing reduced adipocyte size is the major effect of t10c12 CLA (1, 4, 9). Some studies have found indications of apoptosis (18, 34, 50), although the percentage of the cells lost from the tissues was not established in those studies. We observed a 47% loss of total cells present in the WAT when the tissue lost 75% or more of its mass. The extent of cell loss may depend on the extent of WAT mass loss, which also varied between studies (reviewed in Refs. 22 and 35). CLA has been reported to inhibit preadipocyte differentiation in 3T3-L1 cells (3, 27), possibly causing the observed adipocyte loss through the lack of replacement of older adipocytes. The reduction in the transcript levels of many key adipocyte differentiation factors such as PPAR-γ and C/EBP-α is likely to prevent preadipocytes from differentiating (12) although we did not see an accumulation of the Pref-1 transcript that is diagnostic of preadipocytes (44). Transcripts of genes involved in apoptotic pathways were found to be both increased and decreased with no clear conclusion about the activity of these pathways apparent from the changes in transcript levels alone. This may be due in part to the different cell types in the WAT and in part to the posttranscriptional nature of the major part of the apoptosis machinery.

Changes in Energy Import, Biosynthesis, and Storage

Two major sources of metabolites that are converted and stored in the adipocytes' lipid droplet are glucose, imported via the insulin sensitive glucose transporter system, and fatty acids, available from the hydrolysis of extracellular VLDL bound triglycerides via lipoprotein lipase (32). Our results agree with and extend previous reports showing a large decrease in transcripts for genes responsible for glucose and fatty acid uptake (21), including the insulin-sensitive glucose transporter gene GLUT4 (9), the facilitated glucose/fructose transporter member SLC2A5, and numerous genes for biosynthesis of fatty acids (Table 4). Additionally, most of the transcripts involved with anabolic processes such as gluconeogenesis, citrate acid cycle, fatty acid metabolism, proprionate, buturonate, and sterol biosynthesis were strongly downregulated (Tables 3 and 4), indicating a greatly reduced capacity for the biosynthesis of fatty acids and sterols. This is consistent with the increased insulin resistance observed in many studies in CLA-fed mice (reviewed in Ref. 22) and is in agreement with the experimental observations demonstrating uptake of glucose and fatty acids is reduced in cultured human adipocytes (4).

Additional genes with reduced mRNA levels that are expected to reduce TG synthesis include a key subunit of acylation-stimulating protein (31), caveolin I (41), and *Lipn1* (39). Recent studies with the yeast *lipn1* homolog PAH1 and mammalian LIPN1 protein indicate they have a phosphatidate phosphatase activity that regulates the flow of phospholipids into membranes or TAG production (15). When the PAH1 protein is absent or phosphorylated, an excess of phospholipids and reduced amounts of TAG are produced. This new biochemical role of LIPN1 may indirectly account for gene expression changes previously considered to be a direct regulatory affect on transcription (15, 42). The reduction in the mRNA levels for the carbohydrate responsive element binding

protein (ChREBP) is also a likely factor because ChREBP-deficient mice show symptoms of reduced adiposity and down-regulation of lipid biosynthetic enzymes (23).

Increased Energy Expenditure

Evidence suggesting an increased cellular energy expenditure in RP tissues is the 26- and 4-fold increase in mRNA levels for UCP1 and UCP2, respectively. Similar results of increased UCP1 or UCP2 transcript or activity levels have been observed in some (18) but not other studies of CLA-fed mice (21, 53, 54). UCP1 plays a role in mitochondrial energy expenditure, whereas UCP2's role is still emerging and appears not to be involved in thermogenesis (29, 43). Further supporting a possible increase in cellular energy expenditure was the increase in CPT1 mRNA. CPT1 is considered a rate-limiting step in fatty acid beta-oxidation in the mitochondria (2) and has been previously observed to increase in CLA-fed mice (36) and rats (30). CLA-fed mice have been reported to have an increased energy expenditure, and 74% of the energy loss was found to be due to increased metabolic heat output (49). The large UCP1 and CPT1 transcript increases observed in this study and by others (21, 22) suggest that caloric energy expenditure via mitochondrial heat loss in the WAT of the t10c12 CLA-fed mice is occurring. The reduced mRNA levels of regulatory factor Rip140 observed may be part of the mechanism responsible as mice knockouts of this gene show increased UCP1 and CPT1 levels (7, 40).

Energy Export

Lipolysis of the TGs in the lipid droplet and export of free fatty acids and glycerol make up the major means of energy export from living adipocytes. An increased rate of lipolysis has been reported for cultured adipocytes (5), but no increase in rate was found in CLA-fed mice (55). The two- to sevenfold declines in the levels of the transcripts of the key lipolytic enzymes involved in fatty acid transport out of in t10c12 CLA-treated adipocytes indicate a reduced rate of hydrolysis is likely occurring, but some residual hydrolytic activity is likely as these transcripts are still in the 90th percentile of the most abundant mRNA signals.

Signaling and Inflammation

The current limited understanding of the initial molecular responses to t10c12 CLA include a desaturation step by a delta-six desaturase that is required to produce an active t10c12 CLA metabolite (16), activation of a PTX-sensitive GPCR, activation of the U1026-sensitive MEK/ERK pathway, activation of kamebakaurin-sensitive NF-κB pathway, and induction of IL-6 (4). IL-6 was necessary for the CLA response in cultured human adipocytes (4) and was highly induced 24 h after t10c12 CLA treatment in the present analysis. Its levels declined to normal values after 48 h. The role TNF-α plays is unclear (8), and TNF-α mRNA levels increased by 20% or less in our experiments. A transient increase in TNF-α was observed at 3 h after CLA treatment in cultured human adipose cells (8) and might have subsided before our earliest time point at 24 h. Evidence for IL-1β as a means to activate NF-κB was the sustained upregulation of IL-1β- and IL-1β-induced genes CASP1, CASP IV, and PTX3 (Table 8). Either TNF-α or IL-1β signals are capable of activating NF-κB via the NF-κB kinase. Activated NF-κB and ERK1/2 may constitute key steps to induce the inflammatory response (8), including IL-6 induction and reduction of PPAR-γ activity, one of the key adipocyte regulatory proteins (33). The mRNA levels increased for some members of the NF-κB family including IκBKB, IκBKG, and the inhibitors of NF-κB activation, NFκBIA and NFκBIB, possibly due to feedback mechanisms to regulate the inflammatory responses. Our microarray analyses are consistent with activation of these pathways, particularly with the large changes in cytokine transcript levels described below.

The numerous cytokines transcripts that change in abundance in response to t10c12 CLA feeding can be organized into two classes (Table 8): *1*) those secreted factors associated with endocrine and paracrine functions that declined, including leptin, resistin, adiponectin, adipsin, and visfatin; and *2*) the >50 mRNAs associated with inflammation that increased, including IL-1, 6, 10, 15, and 17, and the receptors IL1RN, IRAKB, ILR1, IL10R, IL10RA, IL10RB, IL17R, IL13R, IL13RA, and IL2RT. Additionally, the transcripts increased for >30 of the CXC and CC ligand family of cytokines and extracellular factors (CCL7 or MCP-7), CCL4 or MPlB (Table 8 and Supplemental Table 4).

Summary

One limitation of WAT mRNA transcript array data is that it averages the transcript abundance across the several major cell types in WAT including adipocytes, stromal-vascular and connective fibroblasts, vascular endothelial cells, and immune cells. Nonetheless several trends are apparent. The t10c12 CLA-mediated mRNA changes suggest that the dynamic equilibrium of fatty acid turnover in WAT (25) could be shifted toward net export because very little import or biosynthesis appears to be occurring while presumably maintaining a reduced export capability. Sustained conditions of very little import and recurring export could result in considerable depletion of the lipid droplet. Together with an increase in cellular energy expenditure, reduced preadipocyte differentiation due to reduction of key regulatory proteins, and cell loss due to apoptosis, these combined changes seemingly account for the severe lipid and tissue loss observed in RP tissues. The surprisingly large contingent of induced cytokine-related genes may accelerate this process.

ACKNOWLEDGMENTS

We thank Alan Doster for help with initial tissue sections.

GRANTS

This work was supported by National Science Foundation Grant EPS-0346476.

REFERENCES

1. **Azain MJ, Hausman DB, Sisk MB, Flatt WP, and Jewell DE.** Dietary conjugated linoleic acid reduces rat adipose tissue cell size rather than cell number. *J Nutr* 130: 1548–1554, 2000.
2. **Bartlett K and Eaton S.** Mitochondrial beta-oxidation. *Eur J Biochem* 271: 462–469, 2004.
3. **Brodie AE, Manning VA, Ferguson KR, Jewell DE, and Hu CY.** Conjugated linoleic acid inhibits differentiation of pre- and post- confluent 3T3–L1 preadipocytes but inhibits cell proliferation only in preconfluent cells. *J Nutr* 129: 602–606, 1999.
4. **Brown JM, Boysen MS, Chung S, Fabiyi O, Morrison RF, Mandrup S, and McIntosh MK.** Conjugated linoleic acid induces human adipocyte

delipidation: autocrine/paracrine regulation of MEK/ERK signaling by adipocytokines. *J Biol Chem* 279: 26735–26747, 2004.

5. **Brown JM and McIntosh MK.** Conjugated linoleic acid in humans: regulation of adiposity and insulin sensitivity. *J Nutr* 133: 3041–3046, 2003.
6. **Calvano SE, Xiao W, Richards DR, Felciano RM, Baker HV, Cho RJ, Chen RO, Brownstein BH, Cobb JP, Tschoeke SK, Miller-Graziano C, Moldawer LL, Mindrinos MN, Davis RW, Tompkins RG, Lowry SF, and Inflamm and Host Response to Injury Large Scale Collab. Res. Program.** A network-based analysis of systemic inflammation in humans. *Nature* 437: 1032–1037, 2005.
7. **Christian M, Kiskinis E, Debevec D, Leonardsson G, White R, and Parker MG.** RIP140-targeted repression of gene expression in adipocytes. *Mol Cell Biol* 25: 9383–9391, 2005.
8. **Chung S, Brown JM, Provo JN, Hopkins R, and McIntosh MK.** Conjugated linoleic acid promotes human adipocyte insulin resistance through NFkappaB-dependent cytokine production. *J Biol Chem* 280: 38445–38456, 2005.
9. **Chung S, Brown JM, Sandberg MB, and McIntosh M.** Trans-10,cis-12 CLA increases adipocyte lipolysis and alters lipid droplet-associated proteins: role of mTOR and ERK signaling. *J Lipid Res* 46: 885–895, 2005.
10. **DeLany JP, Blohm F, Truett AA, Scimeca JA, and West DB.** Conjugated linoleic acid rapidly reduces body fat content in mice without affecting energy intake. *Am J Physiol Regul Integr Comp Physiol* 276: R1172–R1179, 1999.
11. **Evans M, Geigerman C, Cook J, Curtis L, Kuebler B, and McIntosh M.** Conjugated linoleic acid suppresses triglyceride accumulation and induces apoptosis in 3T3–L1 preadipocytes. *Lipids* 35: 899–910, 2000.
12. **Evans M, Park Y, Pariza M, Curtis L, Kuebler B, and McIntosh M.** Trans-10,cis-12 conjugated linoleic acid reduces triglyceride content while differentially affecting peroxisome proliferator activated receptor gamma2 and aP2 expression in 3T3–L1 preadipocytes. *Lipids* 36: 1223–1232, 2001.
13. **Gautier L, Cope L, Bolstad BM, and Irizarry RA.** affy–analysis of Affymetrix GeneChip data at the probe level. *Bioinformatics* 20: 307–315, 2004.
14. **Gijbels MJJ, van der Cammen M, van der Laan LJW, Emeis JJ, Havekes LM, Hofker MH, and Kraal G.** Progression and regression of atherosclerosis in APOE3-Leiden transgenic mice: an immunohistochemical study. *Atherosclerosis* 143: 15–25, 1999.
15. **Han GS, Wu WI, and Carman GM.** The *Saccharomyces cerevisiae* lipin homolog is a Mg^{2+}-dependent phosphatidate phosphatase enzyme. *J Biol Chem* 281: 9210–9218, 2006.
16. **Hargrave KM, Azain MJ, and Miner JL.** Dietary coconut oil increases conjugated linoleic acid-induced body fat loss in mice independent of essential fatty acid deficiency. *Biochim Biophys Acta* 1737: 52–60, 2005.
17. **Hargrave KM, Li C, Meyer BJ, Kachman SD, Hartzell DL, Della-Fera MA, Miner JL, and Baile CA.** Adipose depletion and apoptosis induced by trans-10, cis-12 conjugated linoleic acid in mice. *Obes Res* 10: 1284–1290, 2002.
18. **Hargrave KM, Meyer BJ, Li C, Azain MJ, Baile CA, and Miner JL.** Influence of dietary conjugated linoleic acid and fat source on body fat and apoptosis in mice. *Obes Res* 12: 1435–1444, 2004.
19. **Harris SL and Levine AJ.** The p53 pathway: positive and negative feedback loops. *Oncogene* 24: 2899–2908, 2005.
20. **Holness CL and Simmons DL.** Molecular cloning of CD68, a human macrophage marker related to lysosomal glycoproteins. *Blood* 81: 1607–1613, 1993.
21. **House RL, Cassady JP, Eisen EJ, Eling TE, Collins JB, Grissom SF, and Odle J.** Functional genomic characterization of delipidation elicited by trans-10, cis-12-conjugated linoleic acid (t10c12-CLA) in a polygenic obese line of mice. *Physiol Genomics* 21: 351–361, 2005.
22. **House RL, Cassady JP, Eisen EJ, McIntosh MK, and Odle J.** Conjugated linoleic acid evokes de-lipidation through the regulation of genes controlling lipid metabolism in adipose and liver tissue. *Obes Rev* 6: 247–258, 2005.
23. **Iizuka K, Bruick RK, Liang G, Horton JD, and Uyeda K.** Deficiency of carbohydrate response element-binding protein (ChREBP) reduces lipogenesis as well as glycolysis. *Proc Natl Acad Sci USA* 101: 7281–7286, 2004.
24. **Irizarry RA, Hobbs B, Collin F, Beazer-Barclay YD, Antonellis KJ, Scherf U, and Speed TP.** Exploration, normalization, and summaries of high density oligonucleotide array probe level data. *Biostatistics* 4: 249–264, 2003.
25. **Kalderon B, Mayorek N, Berry E, Zevit N, and Bar-Tana J.** Fatty acid cycling in the fasting rat. *Am J Physiol Endocrinol Metab* 279: E221–E227, 2000.
26. **Kanda H, Tateya S, Tamori Y, Kotani K, Hiasa K, Kitazawa R, Kitazawa S, Miyachi H, Maeda S, Egashira K, and Kasuga M.** MCP-1 contributes to macrophage infiltration into adipose tissue, insulin resistance, and hepatic steatosis in obesity. *J Clin Invest* 116: 1494–1505, 2006.
27. **Kang K, Liu W, Albright KJ, Park Y, and Pariza MW.** Trans-10,cis-12 CLA inhibits differentiation of 3T3–L1 adipocytes and decreases PPAR gamma expression. *Biochem Biophys Res Commun* 303: 795–799, 2003.
28. **Khazen W, M'Bika JP, Tomkiewicz C, Benelli C, Chany C, Achour A, and Forest C.** Expression of macrophage-selective markers in human and rodent adipocytes. *FEBS Lett* 579: 5631–5634, 2005.
29. **Krauss S, Zhang CY, and Lowell BB.** The mitochondrial uncoupling-protein homologues. *Nat Rev Mol Cell Biol* 6: 248–261, 2005.
30. **Martin JC, Gregoire S, Siess MH, Genty M, Chardigny JM, Berdeaux O, Juaneda P, and Sebedio JL.** Effects of conjugated linoleic acid isomers on lipid-metabolizing enzymes in male rats. *Lipids* 35: 91–98, 2000.
31. **Maslowska M, Legakis H, Assadi F, and Cianflone K.** Targeting the signaling pathway of acylation stimulating protein. *J Lipid Res* 47: 643–652, 2006.
32. **Mead J, Irvine S, and Ramji D.** Lipoprotein lipase: structure, function, regulation, and role in disease. *J Mol Med* 80: 753, 2002.
33. **Miard S and Fajas L.** Atypical transcriptional regulators and cofactors of PPARgamma. *Int J Obes (Lond)* 29, *Suppl* 1: S10–S12, 2005.
34. **Miner JL, Cederberg CA, Nielsen MK, Chen X, and Baile CA.** Conjugated linoleic acid (CLA), body fat, and apoptosis. *Obes Res* 9: 129–134, 2001.
35. **Pariza MW, Park Y, and Cook ME.** The biologically active isomers of conjugated linoleic acid. *Prog Lipid Res* 40: 283–298, 2001.
36. **Park Y, Albright KJ, Liu W, Storkson JM, Cook ME, and Pariza MW.** Effect of conjugated linoleic acid on body composition in mice. *Lipids* 32: 853–858, 1997.
37. **Peterfy M, Phan J, and Reue K.** Alternatively spliced lipin isoforms exhibit distinct expression pattern, subcellular localization, and role in adipogenesis. *J Biol Chem* 280: 32883–32889, 2005.
38. **Peterfy MPJ, Xu P, Reue K.** Lipodystrophy in the fld mouse results from mutation of a new gene encoding a nuclear protein, lipin. *Nat Genet* 27: 121–124, 2001.
39. **Poirier H, Niot I, Clement L, Guerre-Millo M, and Besnard P.** Development of conjugated linoleic acid (CLA)-mediated lipoatrophic syndrome in the mouse. *Biochimie* 87: 73–79, 2005.
40. **Powelka AM, Seth A, Virbasius JV, Kiskinis E, Nicoloro SM, Guilherme A, Tang X, Straubhaar J, Cherniack AD, Parker MG, and Czech MP.** Suppression of oxidative metabolism and mitochondrial biogenesis by the transcriptional corepressor RIP140 in mouse adipocytes. *J Clin Invest* 116: 125–136, 2006.
41. **Razani B, Combs TP, Wang XB, Frank PG, Park DS, Russell RG, Li M, Tang B, Jelicks LA, Scherer PE, and Lisanti MP.** Caveolin-1-deficient mice are lean, resistant to diet-induced obesity, and show hypertriglyceridemia with adipocyte abnormalities. *J Biol Chem* 277: 8635–8647, 2002.
42. **Reue K and Donkor J.** Lipin: a determinant of adiposity, insulin sensitivity and energy balance. *Future Lipidology* 1: 91–101, 2006.
43. **Ricquier D.** Respiration uncoupling and metabolism in the control of energy expenditure. *Proc Nutr Soc* 64: 47–52, 2005.
44. **Smas CM and Sul HS.** Pref-1, a protein containing EGF-like repeats, inhibits adipocyte differentiation. *Cell* 73: 725–734, 1993.
45. **Smyth GK.** Linear models and empirical bayes methods for assessing differential expression in microarray experiments. *Stat Appl Genet Mol Biol* 3: Article 3, 2004.
46. **Smyth GK, Michaud J, and Scott H.** The use of within-array replicate spots for assessing differential expression in microarray experiments. *Bioinformatics* 21: 2067–2075, 2005.
47. **Takahashi Y, Kushiro M, Shinohara K, and Ide T.** Dietary conjugated linoleic acid reduces body fat mass and affects gene expression of proteins regulating energy metabolism in mice. *Comp Biochem Physiol B Biochem Mol Biol* 133: 395–404, 2002.

48. **Terpstra AH, Javadi M, Beynen AC, Kocsis S, Lankhorst AE, Lemmens AG, and Mohede IC.** Dietary conjugated linoleic acids as free fatty acids and triacylglycerols similarly affect body composition and energy balance in mice. *J Nutr* 133: 3181–3186, 2003.
49. **Terpstra AHM, Beynen AC, Everts H, Kocsis S, Katan MB, and Zock PL.** The decrease in body fat in mice fed conjugated linoleic acid is due to increases in energy expenditure and energy loss in the excreta. *J Nutr* 132: 940–945, 2002.
50. **Tsuboyama-Kasaoka N, Takahashi M, Tanemura K, Kim HJ, Tange T, Okuyama H, Kasai M, Ikemoto S, and Ezaki O.** Conjugated linoleic acid supplementation reduces adipose tissue by apoptosis and develops lipodystrophy in mice. *Diabetes* 49: 1534–1542, 2000.
51. **Wang Y and Jones PJ.** Dietary conjugated linoleic acid and body composition. *Am J Clin Nutr* 79: 1153S–1158S, 2004.
52. **Wang YW and Jones PJ.** Conjugated linoleic acid and obesity control: efficacy and mechanisms. *Int J Obes Relat Metab Disord* 28: 941–955, 2004.
53. **West DB, Blohm FY, Truett AA, and DeLany JP.** Conjugated linoleic acid persistently increases total energy expenditure in AKR/J mice without increasing uncoupling protein gene expression. *J Nutr* 130: 2471–2477, 2000.
54. **West DB, Delany JP, Camet PM, Blohm F, Truett AA, and Scimeca J.** Effects of conjugated linoleic acid on body fat and energy metabolism in the mouse. *Am J Physiol Regul Integr Comp Physiol* 275: R667–R672, 1998.
55. **Xu X, Storkson J, Kim S, Sugimoto K, Park Y, and Pariza MW.** Short-term intake of conjugated linoleic acid inhibits lipoprotein lipase and glucose metabolism but does not enhance lipolysis in mouse adipose tissue. *J Nutr* 133: 663–667, 2003.